

## Metal–Metal Bonding

Deutsche Ausgabe: DOI: 10.1002/ange.201605543  
Internationale Ausgabe: DOI: 10.1002/anie.201605543

## A Family of Multiply Bonded Dimolybdenum Boraamidates with the Formal Mo–Mo Bond Orders of 3, 4, 4.5, and 5

Duan-Yen Lu, Ting-Shen Kuo, and Yi-Chou Tsai\*

Dedicated to Professor Christopher C. Cummins on the occasion of his 50<sup>th</sup> birthday

**Abstract:** A boraamidinato ligand  $[\text{PhB}(\text{N}-2,6\text{-}i\text{Pr}_2\text{C}_6\text{H}_3)_2]^{2-}$  was employed to stabilize a new family of multiply bonded dimolybdenum complexes  $[\text{MoCl}(\mu\text{-}\kappa^2\text{-PhB}(\text{N}-2,6\text{-}i\text{Pr}_2\text{C}_6\text{H}_3)_2)]_2$  (**4**) and  $[\text{Mo}(\mu\text{-}\kappa^2\text{-PhB}(\text{N}-2,6\text{-}i\text{Pr}_2\text{C}_6\text{H}_3)_2)]_2^{n-}$  ( $n=0$  (**5**), 1 (**6**), 2 (**7**)), with the respective formal Mo–Mo bond orders of 3, 4, 4.5, and 5. Each metal center in **5–7** is two-coordinate with respect to the ligands. Of particular interest is the quadruply bonded dimolybdenum complex **5**, featuring an unprecedented angular conformation. The bent  $\text{Mo}_2\text{N}_4$  core of **5** distorts toward planarity upon reduction. As a result, compound **7** features a planar  $\text{Mo}_2\text{N}_4$  core, while that of **6** is still bent but less significantly than that of **5**. Additionally, the Mo–Mo bond lengths of **4–7** systematically decrease as the valency of the central  $\text{Mo}_2$  units decreases. Complex **7** features the shortest Mo–Mo bond length (2.0106(5) Å) yet reported.

The triply and quadruply bonded dinuclear complexes have predominated metal–metal multiple bonding for more than 50 years.<sup>[1]</sup> By contrast, dinuclear complexes with a metal–metal quintuple bond are relatively limited,<sup>[2]</sup> following the recognition of the dimeric chromium complex  $\text{Cr}_2[2,6\text{-}i\text{Pr}_2\text{C}_6\text{H}_3)_2\text{C}_6\text{H}_3]_2$  in 2005.<sup>[3]</sup> In general, these three types of metal–metal multiple bonds exist in three distinct structural configurations. The trigonal arrangement  $\text{M}_2\text{X}_6$  is the most prevalent conformation in the triple bonding structure (Figure 1a).<sup>[1,4,5]</sup> In quadruple bonding, the predominant structural configuration has been tetragonal geometry (Figure 1b) since 1964.<sup>[1]</sup> Although the lantern structure was observed in the case of quintuple bonding,<sup>[6]</sup> all characterized quintuply bonded dinuclear complexes feature the planar conformation, as illustrated in Figure 1c.<sup>[7]</sup>

We are interested in dinuclear complexes that undergo transitions from low to high metal–metal bond orders. For example, we described the characterization of two quintuply bonded dimolybdenum amidinates  $[\text{Mo}(\mu\text{-}\kappa^2\text{-RC}(\text{N}-2,6\text{-}i\text{Pr}_2\text{C}_6\text{H}_3)_2)]_2$  ( $\text{R}=\text{H}$  (**1**),  $\text{Ph}$  (**2**))<sup>[7d]</sup> by  $\text{KC}_8$  reduction of

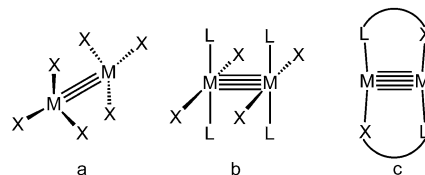


**Figure 1.** The representative structures of the a) triply, b) quadruply, and c) quintuply bonded dinuclear complexes.

their corresponding  $\text{Mo}^{\text{II}}\equiv\text{Mo}^{\text{II}}$  quadruply bonded paddle-wheel species  $\text{Mo}_2(\mu\text{-Cl})[\text{Cl}_2\text{Li}(\text{OEt}_2)][\mu\text{-}\kappa^2\text{-RC}(\text{N}-2,6\text{-}i\text{Pr}_2\text{C}_6\text{H}_3)_2]_2$ . Carmona et al. have shown that **1** can be alternatively generated from the quadruply bonded dihydrido species  $[\text{Mo}(\text{H})(\text{THF})(\mu\text{-}\kappa^2\text{-HC}(\text{N}-2,6\text{-}i\text{Pr}_2\text{C}_6\text{H}_3)_2)]_2$  (THF = tetrahydrofuran) by reductive elimination of  $\text{H}_2$ .<sup>[7a]</sup> Moreover, we reported the first low-coordinate quadruply bonded dimolybdenum complex  $[\text{Mo}(\mu\text{-}\kappa^2\text{-Me}_2\text{Si}(\text{N}-2,6\text{-}i\text{Pr}_2\text{C}_6\text{H}_3)_2)]_2$  (**3**),<sup>[8]</sup> which was synthesized by  $\text{KC}_8$  reduction of its triply bonded dimolybdenum precursor  $\text{syn-}[\text{MoCl}(\mu\text{-}\kappa^2\text{-Me}_2\text{Si}(\text{N}-2,6\text{-}i\text{Pr}_2\text{C}_6\text{H}_3)_2)]_2$  (**3-Cl**). In **3**, the quadruply bonded  $\text{Mo}_2$  unit is spanned by two silicon-bridged diamido ligands and each Mo atom adopts a linear geometry with respect to the ligands. The linear N–Mo–N arrangement is a consequence of strong Mo–N  $\pi$  interactions, on the basis of theoretical calculations. However, attempts to increase the Mo–Mo bond order by adding electrons to **3** was not successful because the LUMO of **3** possesses  $\delta^*$  character.

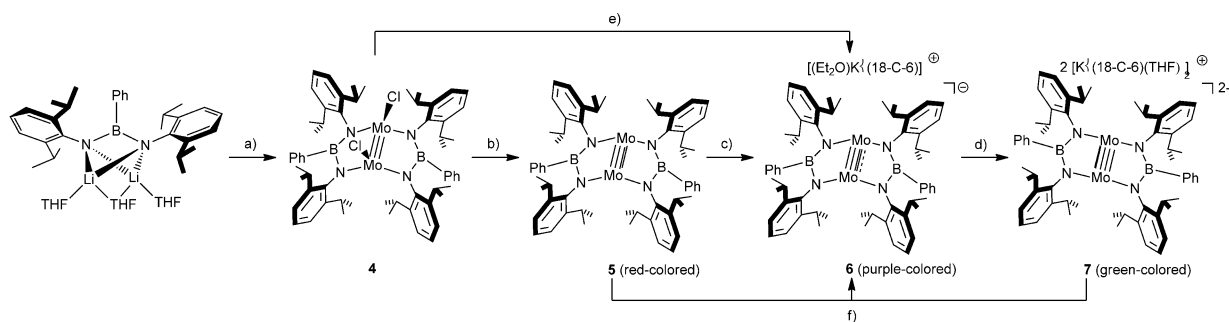
In comparison with the  $\sigma$ -donating amidinates and  $\pi$ -donating  $[\text{Me}_2\text{Si}(\text{N}-2,6\text{-}i\text{Pr}_2\text{C}_6\text{H}_3)_2]^{2-}$ , we expected that the employment of the less  $\pi$ -donating boraamidinate  $[\text{PhB}(\text{N}-2,6\text{-}i\text{Pr}_2\text{C}_6\text{H}_3)_2]^{2-}$ <sup>[9]</sup> stabilizes the multiply bonded  $\text{Mo}_2$  units. Herein, we describe the characterization of an unprecedented  $\text{Mo}\equiv\text{Mo}$  quadruple bond in an angular compound supported by two boraamidates, from which two dimolybdenum compounds with the formal Mo–Mo bond orders of 4.5 and 5 were subsequently prepared.

As illustrated in Scheme 1, a metathesis reaction between the dilithio boraamidinate  $(\text{THF})_3\text{Li}_2[\text{PhB}(\text{N}-2,6\text{-}i\text{Pr}_2\text{C}_6\text{H}_3)_2]$  and  $\text{MoCl}_3(\text{THF})_3$  afforded the orange–yellow crystalline dimeric molybdenum complex  $\text{syn-}[\text{MoCl}(\mu\text{-}\kappa^2\text{-PhB}(\text{N}-2,6\text{-}i\text{Pr}_2\text{C}_6\text{H}_3)_2)]_2$  (**4**) in an isolated yield of 17.6%. The reducing nature of the ligand is blamed for the low yield of **4**, as evidenced by the observation of free bis(arylamido)phenylborane in the reaction by  $^1\text{H}$  NMR spectroscopy. The full  $^{11}\text{B}$  (a broad signal at 48.3 ppm),  $^{13}\text{C}$ , and  $^1\text{H}$  NMR spectra indicate that **4** possesses  $C_{2v}$  symmetry.

[\*] Dr. D.-Y. Lu, Prof. Dr. Y.-C. Tsai  
Department of Chemistry and Frontier Research Center on Fundamental and Applied Sciences and Matters  
National Tsing Hua University  
101, Sec. 2, Guang-Fu Road, Hsinchu 300 (Taiwan)  
E-mail: yicstai@mx.nthu.edu.tw

T.-S. Kuo  
Department of Chemistry, National (Taiwan) Normal University  
88, Sec. 4, Ting-Chow Rd, Taipei 116 (Taiwan)

Supporting information for this article can be found under:  
<http://dx.doi.org/10.1002/anie.201605543>.



**Scheme 1.** Preparation and chemical reduction of the bent quadruply bonded dimolybdenum complex **5**. Reagents and reaction conditions: a)  $\text{MoCl}_3(\text{THF})_3$ , ether,  $-35^\circ\text{C} \rightarrow \text{RT}$ ; b)  $\text{KC}_8$  (2 equiv), ether,  $-35^\circ\text{C} \rightarrow \text{RT}$ ; c)  $\text{KC}_8/18\text{-C-6}$  (1:1), ether,  $-35^\circ\text{C} \rightarrow \text{RT}$ ; d)  $\text{KC}_8/18\text{-C-6}$  (1:1), ether,  $-35^\circ\text{C} \rightarrow \text{RT}$ ; e)  $\text{KC}_8/18\text{-C-6}$  (3 equiv, 1:1), ether,  $-35^\circ\text{C} \rightarrow \text{RT}$ ; f) complex **5**/complex **7** (1:1),  $-35^\circ\text{C} \rightarrow \text{RT}$ , ether.

The molecular structure of **4** was determined by X-ray crystallography,<sup>[10]</sup> as depicted in Figure S1 (Supporting Information). Akin to the structure of  $3\text{-Cl}_2$ ,<sup>[8]</sup> **4** shows a trigonal lantern geometry, in which the  $\text{Mo}_2$  unit is bridged by two boraamidates and each Mo atom carries one terminal chloride. The two N-Mo-N angles are  $121.8(2)$  and  $123.3(2)^\circ$ . Interesting structural metrics to be noted include, the short N-B distances of  $1.456(7)$ – $1.472(7)$  Å (average distance =  $1.465$  Å), suggesting N-B  $\pi$ -bonding character; the Mo-N bond lengths of  $1.975(4)$ – $1.994(4)$  Å (average distance =  $1.981$  Å), which are in the range of the documented Mo-N separations of the triply bonded dimolybdenum amides.<sup>[1]</sup> The Mo-Mo bond length is  $2.1991(6)$  Å, a typical triple bond,<sup>[1]</sup> which is comparable to that of  $3\text{-Cl}_2$  ( $2.2016(10)$  Å), but is longer than that in the triply bonded dimolybdenum boraamidinate  $\text{Mo}_2[\mu\text{-}\kappa^2\text{-PhB}(\text{NET})_2]_3$  ( $2.1612(6)$  Å).<sup>[11]</sup>

Subsequent  $\text{KC}_8$  reduction of **4** in diethyl ether led to the isolation of the quadruply bonded dimolybdenum species  $[\text{Mo}(\mu\text{-}\kappa^2\text{-PhB}(N\text{-}2,6\text{-iPr}_2\text{C}_6\text{H}_3)_2)]_2$  (**5**) in 56% yield after workup. By NMR spectroscopy, **5** in cyclohexane- $d_{12}$  displayed one single set of isopropyl and phenyl peaks in the  $^1\text{H}$  NMR spectrum, and a single resonance at  $44.7$  ppm in the  $^{11}\text{B}$  NMR spectrum. The molecular structure of **5** was deciphered by X-ray crystallography and is presented in Figure 2. The  $\text{Mo}_2$  unit is spanned by two ligands, akin to complex **3**, and each Mo atom is thus two-coordinate with respect to the ligands. The most salient structural feature is that both of the Mo atoms unexpectedly adopt a bent geometry. Two N-Mo-N angles are  $139.5(2)$  and  $140.0(2)^\circ$ . Moreover, the two five-membered  $\text{BN}_2\text{Mo}_2$  heterocycles display an envelope conformation within which two B atoms occupy *endo* positions, suggesting less  $\pi$ -conjugation between B, N, and Mo atoms. This characteristic is manifested by the enhanced B-N bond distance (the average distance is  $1.450$  Å) and the less significant Mo-N  $\pi$ -interactions (the average distance is  $1.994$  Å) compared to those in **4**. Notably, the Mo-Mo bond length dramatically decreases to  $2.1105(9)$  Å, a typical quadruple bond.<sup>[1,12]</sup>

Considering its unusual angular configuration, the possibility that **5** actually contains two hydrido ligands cannot be excluded. However, experimental and theoretical evidence (see below) rules out this possibility. First, the intermetallic distance of **5** is in the normal range of the  $\text{Mo}\equiv\text{Mo}$  quadruple

bond lengths. Second, characteristic signals of hydride functionalities were not observed in the  $^1\text{H}$  NMR (cyclohexane- $d_{12}$ ) and IR (KBr) spectra of **5**, giving credence to a divalent molybdenum formulation. Furthermore, a chloro-

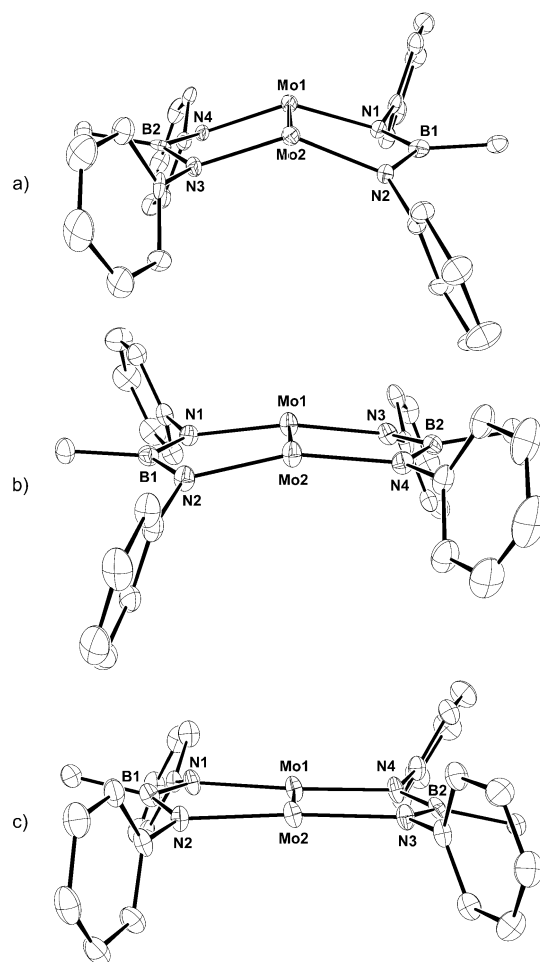


**Figure 2.** The solid-state molecular structures of a) **5**, b) **6**, and c) **7**, where all *i*Pr groups, boron atom-attached phenyl group, hydrogen atoms, and counterions are omitted for the sake of clarity. Selected bond lengths (Å) and angles ( $^\circ$ ): complex **5**; Mo1-Mo2  $2.1104(9)$ , Mo-N  $1.994(5)$  (average), B-N  $1.450(9)$ , N1-Mo1-N4  $140.0(2)$ , N2-Mo2-N3  $139.5(2)$ . Complex **6**; Mo1-Mo2  $2.0548(6)$ , Mo-N  $2.059(4)$  (average), B-N  $1.437(7)$ , N1-Mo1-N4  $160.7(2)$ , N2-Mo2-N3  $161.7(2)$ . Complex **7**; Mo1-Mo2  $2.0106(5)$ , Mo-N  $2.154(4)$  (average), B-N  $1.436(7)$ , N1-Mo1-N4  $166.0(2)$ , N2-Mo2-N3  $170.3(2)$ .

form test<sup>[7a,17b]</sup> was carried out by adding  $\text{CHCl}_3$  or  $\text{CDCl}_3$  to a  $\text{C}_6\text{D}_6$  solution of **5** in a sealed NMR tube, where **4** was rapidly and cleanly formed and  $\text{H}_2$  or HD was not produced, as evidenced by  $^1\text{H}$  NMR spectroscopy.

The bonding schemes in **5** were realized by density functional theory (DFT) calculations at the BP86/def2-TZVP level. The optimized structure also displays a bent conformation with two identical N-Mo-N angles of  $139.3^\circ$  and two puckered  $\text{BMo}_2\text{N}_2$  heterocycles. However, the Mo-Mo bond length ( $2.104 \text{ \AA}$ ) was slightly underestimated and Mo-N (mean =  $2.008 \text{ \AA}$ ) and B-N ( $1.463 \text{ \AA}$ ) distances were overestimated. Analysis of the pattern of the frontier orbitals of the optimized complex **5** suggests a formal  $\text{Mo}\equiv\text{Mo}$  quadruple bond (Supporting Information, Figure S2). Thus, the HOMO at  $-4.47 \text{ eV}$  corresponds to the  $\delta$  component ( $\text{sd}^\pi\delta$ : side-on  $\delta$ -bond) resulting from edge-on overlap of a pair of  $\text{sd}$ -hybridized orbitals (Figure 3a). The HOMO-1 ( $-5.11 \text{ eV}$ ), HOMO-3 ( $-5.61 \text{ eV}$ ), and HOMO-15 ( $-6.30 \text{ eV}$ ) correspond to the  $\sigma$  and two orthogonal  $\pi$  components, respectively. As expected, the  $\pi$ -bonding interactions between two Mo atoms and four N donors are less significant than those in **3**. Of particular interest is that the LUMO ( $-2.92 \text{ eV}$ ; Figure 3a) shows a Mo-Mo  $\delta$ -bonding orbital, which is in sharp contrast to the LUMO ( $\delta^*$ ) of **3**. From **3** and **5**, it appears that the geometry of a two-coordinate quintet  $\text{Mo}^{\text{II}}$  species strongly correlates with the donating property of the supporting ligands. Stabilized by two  $\sigma$ -donors, the divalent molybdenum center favors a bent conformation, but adopts a linear conformation with two  $\pi$ -donors. Notably, the geometries of the two-coordinate quintet divalent mononuclear chromium complexes are ligand-dependent as well, but the bent configuration pre-

dominates.<sup>[13]</sup> Thus far, two-coordinate open-shell divalent heavy transition metal complexes are unprecedented. An absolute quantification of the Mo-Mo bond orders of **5** and **3** were thus made by analyzing the Mayer bond order of 3.53 and 3.50, respectively.

To increase the metal-metal bond order in the quadruply bonded dinuclear complexes without eliminating ligands is currently unprecedented. Since the LUMO of **5** displays Mo-Mo  $\delta$ -bonding character, two equivalents of  $\text{KC}_8$  were then added to **5** in diethyl ether. The color of the solution rapidly changed to dark green via a distinct dark-purple hue. Interestingly, the dark-purple solution remained for at least 12 h upon mixing equimolar amounts of  $\text{KC}_8$  and **5** in diethyl ether. The addition of one equivalent of  $\text{KC}_8$  to the dark-purple solution regenerated the dark-green solution. It became apparent that the dark-purple species is the one-electron reduction product, which was isolated in 40% yield in the form of  $[(\text{Et}_2\text{O})\text{K}\subset 18\text{-C-6}][\textbf{6}]$  (where 18-C-6 is 18-crown-6 ether and **6** is  $[\text{Mo}_2(\mu\text{-}\kappa^2\text{-PhB}(N\text{-}2,6\text{-}\text{Pr}_2\text{C}_6\text{H}_3)_2)]^-$ ). The dark-green compound is thus the two-electron reduction product,  $[(\text{THF})_2\text{K}\subset 18\text{-C-6}][\textbf{7}]$  (**7** is  $[\text{Mo}_2(\mu\text{-}\kappa^2\text{-PhB}(N\text{-}2,6\text{-}\text{Pr}_2\text{C}_6\text{H}_3)_2)]^{2-}$ ), which was obtained in 16.1% yield after recrystallization from THF. The low isolated yield of **7** is attributed to its extremely reducing nature; it is readily oxidized by a trace amount of dioxygen or moisture. Alternatively, **6** is prepared by mixing **5** and **7** in diethyl ether by a comproportionation route, from which **6** is isolated in a quantitative yield after the removal of solvent.

Compound **7** is a diamagnetic species; the  $^1\text{H}$  NMR spectrum of **7** in THF displayed one set of signals corresponding to the ligand environment. Compared to **5**,  $^{11}\text{B}$  NMR spectroscopy showed that the two boron atoms

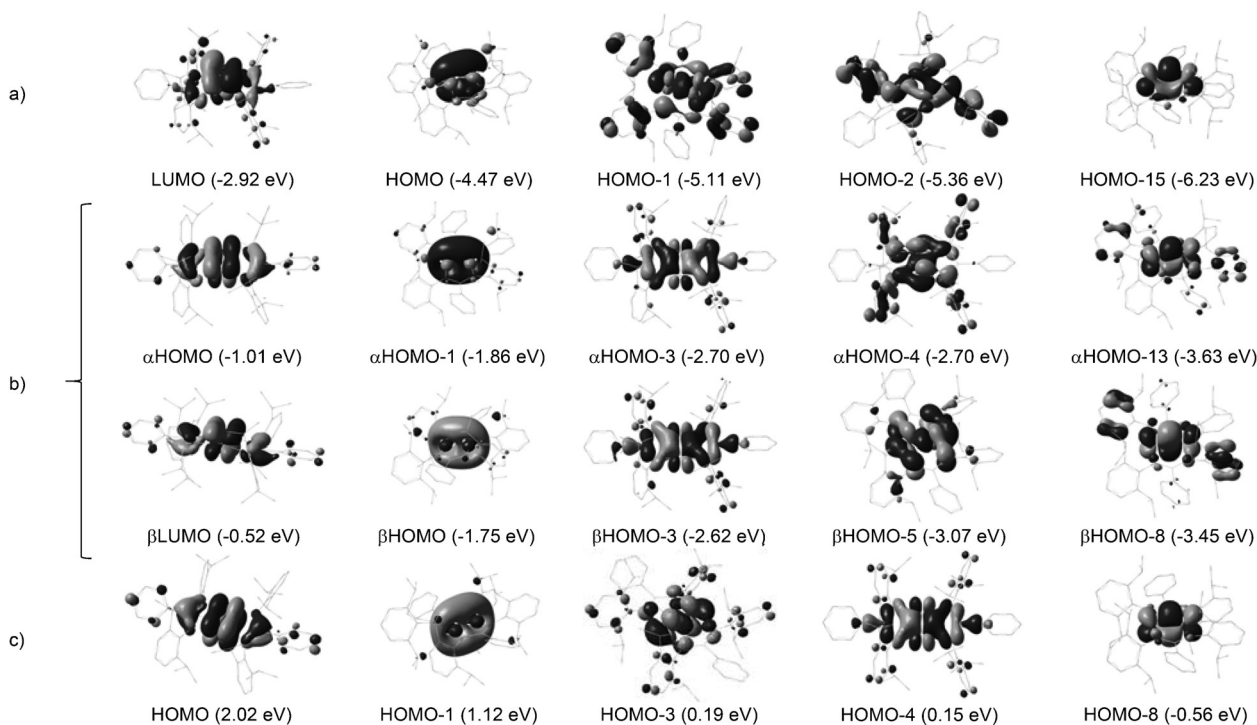


**Figure 3.** The frontier molecular orbitals signifying  $\delta$ ,  $\pi$ , and  $\sigma$  bonding of a)  $[\text{Mo}_2(\mu\text{-}\kappa^2\text{-PhB}(N\text{-}2,6\text{-}\text{Pr}_2\text{C}_6\text{H}_3)_2)_2]$  (**5**), b)  $[\text{Mo}_2(\mu\text{-}\kappa^2\text{-PhB}(N\text{-}2,6\text{-}\text{Pr}_2\text{C}_6\text{H}_3)_2)]^-$  (**6**), and c)  $[\text{Mo}_2(\mu\text{-}\kappa^2\text{-PhB}(N\text{-}2,6\text{-}\text{Pr}_2\text{C}_6\text{H}_3)_2)]^{2-}$  (**7**).



are more magnetically shielded, and their resonance absorption appears at 34.8 ppm. On the other hand, **6** is a paramagnetic species, as expected. The solution magnetic moment determined by the Evans NMR method is  $1.59\mu_{\text{B}}$ , in accordance with possession of one unpaired electron, which prompted us to investigate the radical nature of **6** by EPR spectroscopy. The room temperature EPR spectrum of **6** reveals that the complex is highly reactive in diethyl ether at 294 K. It quickly underwent oxidation (with a trace amount of dioxygen/moisture) to yield unidentified species, even in a freshly prepared diethyl ether solution, as evidenced by gradual decay of its signal over the course of measurement (Supporting Information, Figure S3b). Both experimental and simulated EPR spectra are depicted in Figure S3a (Supporting Information). The spectrum of **6** exhibits resolved superhyperfine structure resulting from interaction of the unpaired spin with the two boron atoms and the four nitrogen atoms with an isotropic signal at  $g_{\text{iso}} = 2.0085$ . As described in detailed EPR studies of the tetragonal dimolybdenum species with a Mo–Mo formal bond order of 3.5, the  $g$ -values vary greatly with oxidation states of the Mo<sub>2</sub> units.<sup>[14]</sup> Mo<sub>2</sub>(II, III) paddlewheel complexes featured  $g$ -values less than 1.950. Yet a larger  $g$ -value of 2.05 was obtained from the Mo<sub>2</sub>(I, II) complex [Mo<sub>2</sub>(CCSiMe<sub>3</sub>)<sub>4</sub>(PMe<sub>3</sub>)<sub>4</sub>]<sup>−</sup>.<sup>[15]</sup> Furthermore, the X-band EPR spectrum (Figure 4) of **6** in frozen diethyl ether at 77 K is characteristic of a spin-doublet state with an axial spin distribution,  $g_2 = g_3 = 1.9445$  and  $g_1 = 2.1327$ . The EPR data for **6** suggest that a single unpaired electron resides in an orbital (the  $d_{xy}$ - $d_{xy}$   $\delta$  orbital) perpendicular to the  $z$ -axis (coincident with the Mo–Mo axis), supported by DFT spin-density calculations (Supporting Information, Figure S4).

X-ray crystallography was used to interrogate the molecular structures of **6** and **7**. As depicted in Figure 2, the central Mo<sub>2</sub>N<sub>4</sub> core in **6** still exhibits a bent conformation. However, this is less significant than **5**, as evidenced by the two N–Mo–N angles of 160.7(2) and 161.7(2)°. As expected, the central Mo<sub>2</sub>N<sub>4</sub> core of **7** is planar, as revealed by the two N–Mo–N angles of 166.0(2) and 170.3(2)°. Moreover, the average Mo–N bond lengths in **5–7** increase as the charges of the Mo<sub>2</sub> moieties decrease, as indicated by the values of 2.059 and 2.154 Å for **6** and **7**, respectively. The mean Mo–N bond

length displays a 3.3% increase from **5** to **6**, and a 4.6% increase from **6** to **7**. By contrast, the Mo–Mo bond lengths regularly decrease to 2.0548(6) (**6**) and 2.0106(5) Å (**7**). Given the Mo≡Mo quadruple bond lengths in the normal range of 2.06–2.17 Å,<sup>[12]</sup> the Mo–Mo distance of **6** is at the lower limit of the range. The shortest documented Mo–Mo bond length is 2.0157(4) Å in **2** (determined by X-ray crystallography),<sup>[7d]</sup> so the extremely short Mo–Mo distance in **7** unambiguously indicates the formation of a quintuple bond.

To corroborate the observed structural metrics of **6** and **7**, and understand their bonding schemes, we performed DFT calculations on the two anions at the BP86/def2-TZVP level. Each computed structure exhibits two identical N–Mo–N angles, 162.7° (**6**) and 168.2° (**7**). The mean Mo–N bond length 2.085 Å of **6** is slightly overestimated, whereas the average Mo–N separation (2.136 Å) of **7** is underestimated. Two slightly different Mo–N Mayer bond orders of 0.65 and 0.62 are obtained for **6**, and the Mo–N Mayer bond order of **7** is 0.57. The decreasing Mo–N bond orders from **5** to **7** reveal that their ionic bonding character increases as the charges of the complexes decrease, and the involvement of Mo  $d$  orbitals in the Mo–N bonding diminishes. Notably, the computed Mo–Mo distances of 2.055 (**6**) and 2.021 Å (**7**) show excellent agreement with the experimental values. The frontier molecular orbitals for **6** and **7** are shown in Figure S2 (Supporting Information). For compound **6**, we see that the  $\alpha$ HOMO at about  $-1.0$  eV does indeed exhibit Mo<sub>2</sub> $\delta$ -bonding character, concomitant with out-of-phase N–B–N  $\pi$ -conjugation. Below the  $\alpha$ HOMO lies another Mo<sub>2</sub> $\delta$  molecular orbital (the  $\alpha$ HOMO–1). Notably, the  $\alpha$ HOMO–1 and  $\alpha$ LUMO respectively correspond to the HOMO and LUMO + 1 in **5**. The  $\alpha$ HOMO–1 ( $-1.86$  eV) and  $\alpha$ LUMO ( $-0.13$  eV) are the Mo<sub>2</sub> $\delta$  and Mo<sub>2</sub> $\delta^*$  molecular orbitals, respectively. The  $\alpha$ LUMO + 1 (0.50 eV) shows Mo<sub>2</sub> $\delta^*$  with out-of-phase Mo–N  $\pi^*$  interactions. Thus, the formal Mo–Mo bond order in **6** is 4.5, although the Mayer bond order calculations gave an output of 3.74. A dinuclear compound with a formal metal–metal bond order of 4.5 is scarce compared to the numerous quadruply and many quintuply bonded dinuclear compounds. A single structurally characterized example is the lantern Cr<sub>2</sub>(I, II) complex [Cr<sub>2</sub>{HC(N-2,6-Me<sub>2</sub>C<sub>6</sub>H<sub>3</sub>)<sub>2</sub>}<sub>3</sub>].<sup>[6c]</sup> As for **7**, we see that the HOMO (Mo<sub>2</sub> $\delta$ ) at 2.02 eV results from subsequent addition of one electron to the  $\beta$ LUMO (Mo<sub>2</sub> $\delta$ ) of **6**. However, it is interesting to note that after one-electron reduction, the pair of  $\alpha$ LUMO + 1 and  $\beta$ LUMO + 4 of Mo<sub>2</sub> $\delta^*$  character in **6** is raised in energy to the LUMO + 13 (4.00 eV) in **7**, displaying an admixture of Mo<sub>2</sub> $\delta^*$  and ligand  $\pi^*$  combination. The formal Mo–Mo bond order of **7** is thus 5, and the calculated Mo–Mo Mayer bond order of 4.17 is comparable to that of **1** (4.24).

In summary, we demonstrated the characterization of a bent quadruply bonded dimolybdenum boraamidinate **5**, which is unprecedented in multiple bonding. Upon reduction of **5**, two dimolybdenum complexes (**6** and **7**) with the formal Mo–Mo bond orders of 4.5 and 5, respectively, were isolated. The success with which these multiply bonded dimolybdenum complexes may be constructed is dominated by electronic effects. A divalent quintet  $d^4$  Mo ion stabilized by two weak

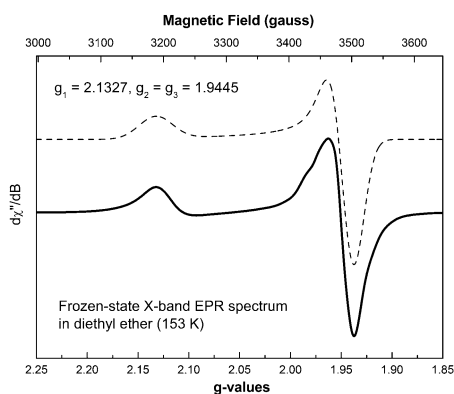


**Figure 4.** The frozen-state X-band EPR spectrum of **6** recorded at 153 K in diethyl ether. Simulated spectrum (-----), experimental spectrum (—).

$\pi$ -donors favors a bent geometry, and a two-coordinate univalent sextet  $d^5$  Mo ion adopts a linear geometry. The low-coordinate quintuply bonded group VI metal dimers have been shown to activate inorganic elements and small molecules,<sup>[16]</sup> and display parallel reactions to unsaturated hydrocarbons.<sup>[17]</sup> Therefore, novel reactivity from each of these new dimolybdenum boraamidates is eagerly anticipated and is currently under study.

## Acknowledgements

We thank the Ministry of Science and Technology (Taiwan) and the Frontier Research Center on Fundamental and Applied Sciences of Matters of National Tsing Hua University for financial support.

**Keywords:** bonding order · boraamidate · molybdenum · multiple bonds ·  $\delta$ -bonds

**How to cite:** *Angew. Chem. Int. Ed.* **2016**, *55*, 11614–11618  
*Angew. Chem.* **2016**, *128*, 11786–11790

- [1] a) F. A. Cotton, L. A. Murillo, R. A. Walton, *Multiple Bonds Between Metal Atoms*, 3rd ed., Springer, Berlin, **2005**; b) Group 6 Metal–Metal Bonds: M. H. Chisholm, N. J. Patmore, in *Molecular Metal–Metal Bonds* (Ed.: S. T. Liddle), Wiley-VCH, Weinheim, **2015**, pp. 139–174.
- [2] a) A. Noor, R. Kempe, *Inorg. Chim. Acta* **2015**, *424*, 75–82; b) A. K. Nair, N. V. S. Harisomayajula, Y.-C. Tsai, *Inorg. Chim. Acta* **2015**, *424*, 51–62; c) A. K. Nair, N. V. S. Harisomayajula, Y.-C. Tsai, *Dalton Trans.* **2014**, *43*, 5618–5638; d) N. V. S. Harisomayajula, A. K. Nair, Y.-C. Tsai, *Chem. Commun.* **2014**, *50*, 3391–3412; e) S.-A. Hua, Y.-C. Tsai, S.-M. Peng, *J. Chin. Chem. Soc.* **2014**, *61*, 9–26; f) F. R. Wagner, A. Noor, R. Kempe, *Nat. Chem.* **2009**, *1*, 529–536.
- [3] T. Nguyen, A. D. Sutton, S. Brynda, J. C. Fetting, G. J. Long, P. P. Power, *Science* **2005**, *310*, 844–847.
- [4] M. H. Chisholm, F. A. Cotton, B. A. Freng, W. W. Reichert, L. W. Shive, B. R. Stults, *J. Am. Chem. Soc.* **1976**, *98*, 4469–4476.
- [5] M. H. Chisholm, F. A. Cotton, M. W. Extine, B. R. Stults, *J. Am. Chem. Soc.* **1976**, *98*, 4477–4485.
- [6] a) L. J. Clouston, R. B. Siedschlag, P. A. Rudd, N. Planas, S. Hu, A. D. Miller, L. Gagliardi, C. C. Lu, *J. Am. Chem. Soc.* **2013**, *135*, 13142–13148; b) S.-C. Liu, W.-L. Ke, J.-S. K. Yu, T.-S. Kuo, Y.-C. Tsai, *Angew. Chem. Int. Ed.* **2012**, *51*, 6394–6397; *Angew. Chem.* **2012**, *124*, 6500–6503; c) Y.-C. Tsai, C.-W. Hsu, J.-S. K. Yu, G.-H. Lee, Y. Wang, T.-S. Kuo, *Angew. Chem. Int. Ed.* **2008**, *47*, 7250–7253; *Angew. Chem.* **2008**, *120*, 7360–7363.
- [7] a) M. Carrasco, N. Curado, C. Maya, R. Peloso, A. Rodríguez, E. Ruiz, S. Álvarez, E. Carmona, *Angew. Chem. Int. Ed.* **2013**, *52*, 3227–3231; *Angew. Chem.* **2013**, *125*, 3309–3313; b) A. Noor, T. Bauer, T. K. Todorova, B. Weber, L. Gagliardi, R. Kempe, *Chem. Eur. J.* **2013**, *19*, 9825–9832; c) Y.-L. Huang, D.-Y. Lu, H.-C. Yu, J.-S. K. Yu, C.-W. Hsu, T.-S. Kuo, G.-H. Lee, *Angew. Chem. Int. Ed.* **2012**, *51*, 7781–7785; *Angew. Chem.* **2012**, *124*, 7901–7905; d) Y.-C. Tsai, H.-Z. Chen, C.-C. Chang, J.-S. K. Yu, G.-H. Lee, Y. Wang, T.-S. Kuo, *J. Am. Chem. Soc.* **2009**, *131*, 12534–12535; e) A. Noor, G. Glatz, R. Müller, M. Kaupp, S. Demeshko, R. Kempe, *Z. Anorg. Allg. Chem.* **2009**, *635*, 1149–1152; f) C.-W. Hsu, J.-S. K. Yu, C.-H. Yen, G.-H. Lee, Y. Wang, Y.-C. Tsai, *Angew. Chem. Int. Ed.* **2008**, *47*, 9933–9936; *Angew. Chem.* **2008**, *120*, 10081–10084; g) A. Noor, F. R. Wagner, R. Kempe, *Angew. Chem. Int. Ed.* **2008**, *47*, 7246–7249; *Angew. Chem.* **2008**, *120*, 7356–7359; h) R. Wolf, C. Ni, T. Nguyen, M. Brynda, G. J. Long, A. D. Sutton, R. C. Fischer, J. C. Fetting, M. Hellman, L. Pu, P. P. Power, *Inorg. Chem.* **2007**, *46*, 11277–11290; i) K. A. Kreisel, G. P. A. Yap, P. O. Dmitrenko, C. R. Landis, K. H. Theopold, *J. Am. Chem. Soc.* **2007**, *129*, 14162–14163.
- [8] Y.-C. Tsai, Y.-M. Lin, J.-S. K. Yu, J.-K. Hwang, *J. Am. Chem. Soc.* **2006**, *128*, 13980–13981.
- [9] T. Chivers, C. Fedorchuk, M. Parvez, *Inorg. Chem.* **2004**, *43*, 2643–2653.
- [10] Detailed crystallographic data for compounds **4–7** is provided in the Supporting Information.
- [11] D. R. Manke, Z.-H. Loh, D. G. Nocera, *Inorg. Chem.* **2004**, *43*, 3618–3624.
- [12] F. A. Cotton, L. M. Daniels, L. M. Hillard, C. A. Murillo, *Inorg. Chem.* **2002**, *41*, 2466–2470.
- [13] a) S. N. König, C. Schädle, C. Maichle-Mössmer, R. Anwander, *Inorg. Chem.* **2014**, *53*, 4585–4597; b) J. N. Boynton, W. A. Merrill, W. M. Reiff, J. C. Fetting, P. P. Power, *Inorg. Chem.* **2012**, *51*, 3212–3219; c) H. Chen, R. A. Bartlett, M. M. Olmstead, P. P. Power, S. C. Shoner, *J. Am. Chem. Soc.* **1990**, *112*, 1048–1055.
- [14] a) F. A. Cotton, L. M. Daniels, L. M. Hillard, C. A. Murillo, *Inorg. Chem.* **2002**, *41*, 1639–1644; b) I.-J. Chang, D. G. Nocera, *J. Am. Chem. Soc.* **1987**, *109*, 4901–4907; c) F. A. Cotton, B. A. Frenz, E. Pedersen, T. R. Webb, *Inorg. Chem.* **1975**, *14*, 391–398.
- [15] K. D. John, T. C. Stoner, M. D. Hopkins, *Organometallics* **1997**, *16*, 4948–4950.
- [16] a) A. Noor, S. Schwarz, R. Kempe, *Organometallics* **2015**, *34*, 2122–2125; b) A. Noor, S. Qayyum, T. Bauer, S. Schwarz, B. Weber, R. Kempe, *Chem. Commun.* **2014**, *50*, 13127–13130; c) P.-F. Wu, S.-C. Liu, Y.-J. Shieh, T.-S. Kuo, G.-H. Lee, Y. Wang, Y.-C. Tsai, *Chem. Commun.* **2013**, *49*, 4391–4393; d) E. S. Tamne, A. Noor, S. Qayyum, T. Bauer, R. Kempe, *Inorg. Chem.* **2013**, *52*, 329–336; e) C. Schwarzmaier, A. Noor, G. Glatz, M. Zabel, A. Y. Timoshkin, B. M. Cossairt, C. C. Cummins, R. Kempe, M. Scheer, *Angew. Chem. Int. Ed.* **2011**, *50*, 7283–7286; *Angew. Chem.* **2011**, *123*, 7421–7424; f) C. Ni, B. D. Ellis, G. J. Long, P. P. Power, *Chem. Commun.* **2009**, 2332–2334.
- [17] a) D.-Y. Lu, P. P.-Y. Chen, T.-S. Kuo, Y.-C. Tsai, *Angew. Chem. Int. Ed.* **2015**, *54*, 9106–9110; *Angew. Chem.* **2015**, *127*, 9234–9238; b) M. Carrasco, N. Curado, E. Álvarez, C. Maya, R. Peloso, M. L. Poveda, A. Rodríguez, E. Ruiz, S. Álvarez, E. Carmona, *Chem. Eur. J.* **2014**, *20*, 6092–6102; c) H.-G. Chen, H.-W. Hsueh, T.-S. Kuo, Y.-C. Tsai, *Angew. Chem. Int. Ed.* **2013**, *52*, 10256–10260; *Angew. Chem.* **2013**, *125*, 10446–10450; d) H.-Z. Chen, S.-C. Liu, C.-H. Yen, J.-S. K. Yu, Y.-J. Shieh, T.-S. Kuo, Y.-C. Tsai, *Angew. Chem. Int. Ed.* **2012**, *51*, 10342–10346; *Angew. Chem.* **2012**, *124*, 10488–10492; e) J. Shen, G. P. A. Yap, J. P. Werner, K. H. Theopold, *Chem. Commun.* **2011**, *47*, 12191–12193; f) A. Noor, E. S. Tamne, S. Qayyum, T. Bauer, R. Kempe, *Chem. Eur. J.* **2011**, *17*, 6900–6903; g) A. Noor, G. Glatz, R. Müller, M. Kaupp, S. Domeschko, R. Kempe, *Nat. Chem.* **2009**, *1*, 322–325.

Received: June 9, 2016

Revised: July 11, 2016

Published online: August 16, 2016